# First Results for a Novel Superconducting Imaging-Surface Sensor Array

**R.H. Kraus, Jr., E.R. Flynn, M. A. Espy, A. Matlashov, W. Overton, M.V. Peters, and P. Ruminer**
Los Alamos National Laboratory, Los Alamos, New Mexico, 87545

*Abstract*— **A superconducting imaging-surface system was constructed using 12 coplanar thin-film SQUID magnetometers located parallel to and spaced 2 cm from a 25 cm diameter lead imaging-plane. Some measurements included two additional sensors on the "back" side of the superconducting imaging-plane to study the field symmetry for our system. Performance was measured in a shielded can and in the open laboratory environment. Data from this system has been used to: (a) understand the noise characteristics of the dewar-SQUID imaging plate arrangement, (b) to verify the imaging principle, (c) measure the background rejection factor of the imaging plane, and (d) compare superconducting materials for the imaging plane.**

**A phantom source field was measured at the sensors as a function of phantom distance from the sensor array to verify the imaging theory. Both the shape and absolute values of the measured and predicted curves agree very well indicating the system is behaving as a gradiometer in accordance with theory. The output from SQUIDs located behind the imaging surface that sense background fields can be used for software or analog background cancellation. Fields arising from sources close to the imaging plane were shielded form the background sensors by more than a factor of 1000. Measurement of the symmetry of sensor sensitivity to uniform fields exactly followed theoretical predictions.**

## I. Introduction

An entirely new multi-channel SQUID gradiometer system, the superconducting imaging-surface gradiometer, based on a novel Los Alamos concept, has been fabricated and tested. A 12-channel system using this design has demonstrated higher performance and lower noise than conventional gradiometer sensor systems. The system also provides additional shielding of background fields, reduced cost, and simpler fabrication techniques than conventional gradiometers. The sensor density and array size can readily be extended, and the geometry of this system is ideal for magnetocardiography (MCG) and related applications.

Current biomagnetic measurements predominantly use gradiometers for almost all applications from magnetoencephalography (MEG) to magnetocardiography (MCG) and magnetoenterography (MEnG), even inside a shielded room. Gradiometer baselines can be tuned to provide maximum signal-to-noise (SNR) sources of interest[1]. Conventional wire-wound gradiometers are, however, both difficult to fabricate with the required precision and difficult to mount in a sensor system. Furthermore, wire wound gradiometers introduce electrical limitations that increase the inherent sensor noise. The superconducting imaging-surface method simplifies gradiometer design considerably.

Manuscript submitted September 15, 1998.
This work was supported by the United States National Institutes of Health (Grant R01-NS31052) and the Department of Energy

The principal application of the array system discussed here is in MCG, while the same superconducting imaging-surface concept is being applied to a whole-head MEG system as well[2]. MCG was first reported in 1963 by Baule and McFee [3] using room temperature pickup coils with several million turns and a ferrite core. The Superconducting Quantum Interference Device (SQUID) was first used for MCG measurements by Cohen et al. [4] in 1969 at MIT. SQUIDs rapidly supplanted room temperature pickup coils for detecting very weak magnetic fields, and are now being used in an ever growing number of applications from biomagnetism and nondestructive testing to geophysical assay and intelligence. Although the extraordinary sensitivity of SQUIDs lowers the threshold for magnetic field sources one can detect, it also increases the sensitivity to noise from ambient field sources requiring the use of shielded rooms and gradiometers[5]. The typical first-order SQUID gradiometer consists of a set of superconducting pickup loops wound in opposition that are sensitive to the difference (derivative) of the field in a specific direction while canceling the uniform component of the field. Winding gradiometer coils requires extraordinary precision to optimize uniform field cancellation (balance) and prevent introducing field distortions. The superconducting imaging method completely avoids this difficulty.

## II. Theory

Fig. 1 depicts both a conventional axial gradiometer coil and a superconducting imaging-surface gradiometer using a flat (planar) imaging surface. Fig. 1a illustrates the currents in a conventional gradiometer coil resulting from the magnetic dipole source shown. Fig. 1b illustrates how the superconducting imaging-surface gradiometer (with a flat imaging surface) responds to both nearby sources and uniform ambient fields. A magnetic source, $M_{source}$, causes Meissner cur-

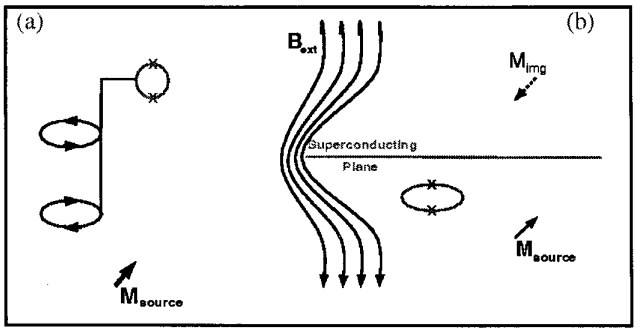


**Figure 1a.** (left) Depiction of conventional wire-wound gradiometer connected to a SQUID and responding to a magnetic source.
**Figure 1b.** (right) Superconducting image-plane gradiometer concept showing a "real" magnetic source, $M_{source}$, and an "image" source, $M_{img}$. See text for detailed description.

rents in the superconductor that can be represented by an image source, $M_{img}$, identical to $M_{source}$ except located behind the imaging plane with opposite sign of the field component perpendicular to the imaging plane. The SQUID magnetometer, shown on the source side of the imaging plane, measures the flux resulting from the superposition of fields from both $M_{source}$ and $M_{img}$. This superposition of fields at the SQUID magnetometer is identical to a gradiometer with one pick-up loop located at the magnetometer, and the second pick-up loop spaced behind the imaging plane at a distance equal to the magnetometer-imaging plane separation. The superconducting surface also provides a natural shield from ambient magnetic fields. Magnetic field lines, $B_{ext}$, are excluded from the superconductor and ambient field lines wrap around the superconductor as shown in Fig. 1b, providing a measure of shielding from ambient fields for sensors relatively close to the plate.

The theory for superconducting imaging gradiometry was first described by van Hulsteyn, et al. [6]. He showed that analytic expressions could only be derived for unconstrained geometries (e.g. those without end). An analytic imaging expression for the flat 12-channel image-surface system must therefore assume an imaging surface of infinite extent. This assumption is justified for magnetic sources where the source-to-imaging-surface distance is much less than the distance from the source to the edge of the imaging surface. Thus, sources that are much closer to the imaging surface and/or the sensor than to the real edge of the imaging surface should be adequately described by the analytic formalism of van Hulsteyn.

The theory holds only for ideal superconductors, consequently any material defects, impurities, or improper cooling of the imaging-surface that would cause significant flux trapping will distort the source image, resulting in an imperfect gradiometer. Therefore, careful consideration must be given to the choice, fabrication, final treatment, and cooling of the imaging surface.

## III. Results

Initial confirmation of the imaging principle was attained using a single channel SQUID with a pickup coil, located in front and behind a five cm diameter lead imaging surface. A gradiometer response was observed for a small source passed in front of the coil with a rejection factor of ~350,000 for uniform fields in a large Helmholtz coil using an analog lock-in amplifier [7].

We have now constructed a flat SQUID-array system utilizing 12 thin-film button SQUIDs that were specifically designed for this effort by Conductus, Inc. in collaboration with and under contract to Los Alamos [6] for use in image-surface systems (Fig. 2). The resulting design integrated both the SQUID circuit and the superconducting pickup loop on a single monolithic device using a niobium lithographic technique. The SQUIDs have extremely low noise characteristics that are extremely stable over time. This button SQUID-magnetometer combined with the source imaging of the superconducting plane generates total fields equivalent to a gradiometer as described above. The result is a axial gradiometer fabricated entirely using a lithographic process, relatively simple and inexpensive to fabricate, and simple to install into sensor arrays. In the present system, we observed 12fT/√Hz at 10 Hz and 10fT/√Hz at 100 Hz noise levels with the system located in a moderately shielded chamber. A flat unshielded noise level of ~1pT/√Hz was observed between ~1Hz and 1kHz in our very (electrically) noisy laboratory.

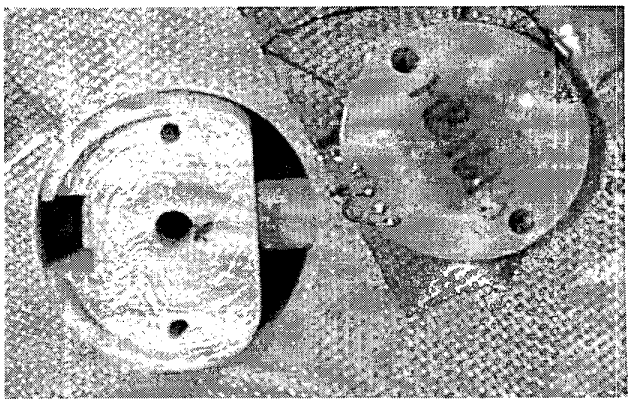

**Figure 2.** Photograph of "Button" SQUID magnetometer (right) and mounting fixture (left).

The SQUID-magnetometers are co-planar and spaced at 2-cm intervals in two rings around a center point as shown in Fig. 3. The inner circle consists of four sensors and the outer circle, eight. The sensors are mounted on cryogenically rated fiberglass tubes that are precisely and rigidly held in place by a spacer disk. This disk maintains the separation and relative parallelism between the sensors and the superconducting disk (the dark layer visible in Fig. 3) between the two fiber-glass

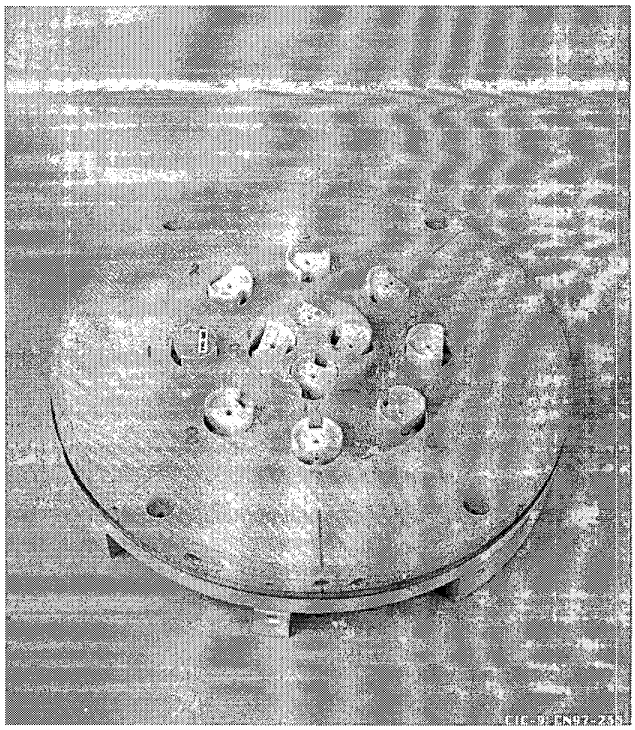

**Figure 3.** Photo of 12 SQUID magnetometer array mounted above superconducting (lead) imaging surface.

disks. Some measurements included two additional sensors on the "back" side of the imaging surface located directly opposite two of the 12 sensors on the "front" (source) side of the imaging plane, one on the inner circle and one on the outer circle. The various configurations of the 12-channel system allowed us to test the essential aspects of the imaging-surface concept including button SQUID-magnetometer performance, imaging surface materials (lead and niobium), and experimental validation of imaging theory.

*A. Button SQUIDs*

The button SQUIDs are located 2 cm from the 25cm diameter imaging-plate resulting in an equivalent 4 cm baseline image-surface gradiometer. The 12-channel system has performed reliably with all channels functional. Data was acquired for performance measurement using the PC-SQUID™ multichannel electronics designed by Conductus for these SQUIDs.

The integrated structure has proven to substantially reduce noise over other magnetometer coils. The field noise we observe for a typical lithographed sensor is 2 to 3 $fT/\sqrt{Hz}$, extremely low for a large area SQUID magnetometer. The transfer function, on the order of 300 $\mu V/\Phi_0$, eliminates the need for a low-temperature matching transformer. The integrated lithographed design also results in a small and simple disc-shaped package containing the entire assembly, as seen in Fig. 2. Four small soldering pads on both sides of the fiberglass disk connect the SQUID device and a heater to the room temperature electronics.

*B. System Measurements*

The theoretically expected shielding factor for this system can be easily estimated as 25/2 = 12.5, the aspect ratio of imaging radius to sensor baseline, at the center of the imaging surface. Thus, background noise in an unshielded environment will only be screened by about a factor of ten and will likely dominate the noise spectra, as we have observed. A phantom was constructed consisting of 12 sets of three orthogonal magnetic dipoles that can be activated by an external signal generator. To verify the imaging theory, the phantom source field was measured at the sensors as a function of phantom distance from the sensor array. Selected

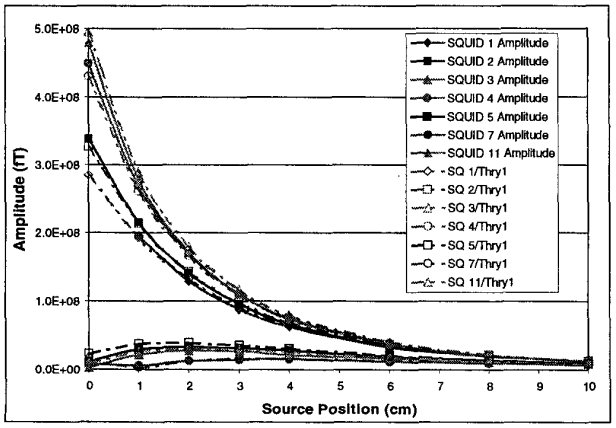


**Figure 4.** Measured SQUID magnetometer sensitivity (dashed) plotted with theoretical gradiometer performance from ref. [4].

sets of these data are shown in Fig. 4 where the measured field at the sensors is plotted as a function of phantom source distance from the imaging plane and compared with the theoretical imaging gradiometer falloff with distance. The data shown are for the $B_z$ phantom that was placed slightly off-center of the pattern of SQUID sensors. The inner ring of sensors were designated SQUID channels 1-4 and the outer ring were channels 5-12 (the labels visible in Fig. 3 do not correlate with the SQUID channel numbers). The data plotted in Fig. 4 are for SQUIDs 1-4, 7, and 11. SQUIDs 1-4 are on the inner ring, closest to the phantom, and the data for these channels is strongly dominated by the $R^{-3}$ term (where R is the imaging plane-phantom source separation). SQUIDs 7 and 11 are on the outer ring, horizontally further away from the phantom, and we find the data for these channels to be dominated by the **M•R** term (see eqn. 5 in [6]). This is a consequence of $\theta$, the angle formed between the phantom source axis and the magnetometer, being large for smaller values of R. As R increases, the $R^{-3}$ term dominates once again and the data from all channels converge.

The data from the channels shown in Fig. 4, as well as all other working channels agree very well with predicted values, indicating the system is behaving as a gradiometer in accordance with theory. Further we observed no deviation from the analytic expressions, for our constrained geometry, even for sources many centimeters away from the imaging surface. Qualitatively, we observed significant deviation from the gradiometric behavior predicted by the analytic formulas only when the phantom source was both near the edge of the imaging plate and spaced away from the surface.

The same measurements shown in Fig. 4 were made for both lead and niobium imaging plates and the same result was obtained for most sensor locations. For one case, however, the plot of measured field as a function of phantom source distance clearly diverted from theory. The noise characteristics and frequency response of the SQUID appeared normal leading us to attribute the variation to an imperfection in the niobium. Inspection of the niobium showed no observable defect in the plate. We conclude that there is no basic difference between type I and type II superconductor performance for this configuration, however there appears to be a greater sensitivity of niobium to inclusions and stresses. The measurements required to determine the observed differences between the lead and niobium imaging surfaces are outside the scope of this effort. Measurements without an imaging plane were difficult because the reduced shielding made it difficult to keep the SQUIDs locked. These measurements could not be made in the shielded can because the field from the phantom coil was severely distorted by eddy current and remnant effects of the shielding can.

We also measured the imaging characteristics of SQUIDs located on the "back" side of the 12-channel flat imaging surface. SQUIDs located behind the imaging surface sense background fields that would be used for software or analog background cancellation. These measurements were performed to determine background sensor sensitivity to phantom sources, and the symmetry of the sensor sensitivity to uniform fields (sensors on the front and back of the

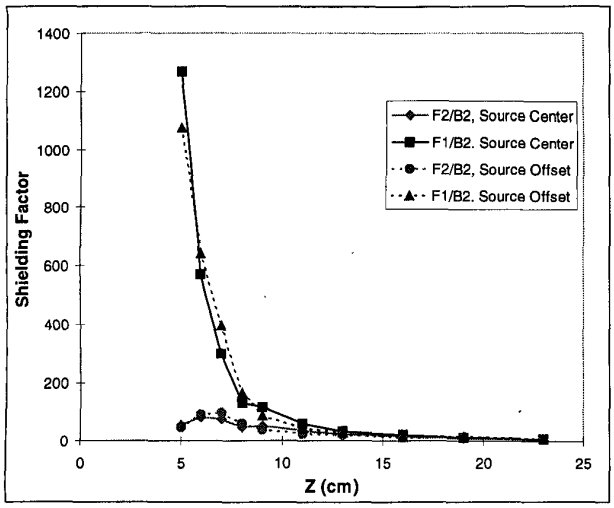


**Figure 5.** Plot of "point-dipole" shielding factors for two different "background" sensors, described in text.

imaging plane should measure the same for a uniform field). Any sensitivity of the background SQUIDs to phantom fields would have the undesirable effect, when software or analog background cancellation was implemented, of canceling a portion of the signal of interest. The symmetry of the sensor sensitivity to uniform fields will be used for developing the analog and software algorithms for background field cancellation and compared with theory at a later date. All measurements reported used the lead imaging plane. Two sensors, B1 and B2, were installed on the back side of the imaging plane. B1 was installed immediately opposite sensor F1 (channel 1) on the inner circle of the 12-channel array, and B2 was installed opposite sensor F5 (channel 5) on the outer circle. The sensitivity ratios between sensors on the front and back of the imaging plane, B1/F1 and B2/F2, are plotted as a function of phantom source distance from the front side of the imaging plane in Figure 5. As expected, the sensitivity of B1 and B2 to the phantom source increases as the separation from the imaging plane increases allowing more field to wrap around the imaging plane to sensors B1 and B2. Figure 5 clearly shows that sources close to the imaging plane are shielded from the background sensors by more than a factor of 1000. Measurements of the source shielding from the background sensors will be used as an additional correction for software background subtraction.

Measurement of the symmetry of sensor sensitivity to uniform fields followed theoretical predictions on the basis of first principles. The field measured in sensors B1 and B2 were equal to the field measured in sensors F1 and F2, respectively, for all field amplitudes and frequencies measured. This observation is dependent on the same imaging characteristics for both sides of the imaging plate and would not hold for geometries other than flat plate. It confirms, however, the fact that the 12-channel imaging plane is operating according to theoretical expectation.

Finally, the system was placed in the uniform field region of a large double Helmholtz coil [7] and the rejection factor for uniform (i.e. distant) fields was measured to be a factor of 11 for the SQUIDs on the inner circle and 8 for those on the outer. These observations very closely match expectations based on first principles.

## IV. Conclusion

We have completed fabrication and preliminary testing of a 12-channel SQUID array using the superconducting image-surface gradiometer concept. Sensor response to "point dipole" magnetic sources, and uniform fields used to simulate ambient magnetic fields followed predicted values to high precision. Edge effects were not observed for sources, within 5cm of the center of the imaging surface independent of whether the source is close or far from the surface. The superconducting imaging-surface also reduced uniform ambient fields at the SQUID sensors by approximately a factor of ten. Finally, a high degree of symmetry was observed between sides of the imaging surface for uniform fields. This symmetry, along with the low sensitivity of sensors on the back side of the imaging-surface to sources close to the front side, provides an excellent circumstance for implementing either digital or analog background rejection.

Our goal is to implement a higher density array with the superconducting imaging surface, together with background rejection, and utilize this system for MCG and other biomagnetic studies.

## References

[1] Garachtchenko, A., Matlachov, A., and Kraus Jr., R.H., "Baseline Distance Optimization for SQUID Gradiometers," IEEE Trans. Applied Superconductivity, (1998, this volume)

[2] Kraus, Jr., R.H., Flynn, E.R., Overton, W., Espy, M.A., Matlashov, A., Peters, M.V., and Ruminer, P., "First Results for a Superconducting Imaging-Surface Sensor Array for Magnetoencephalography," Accepted for pub., Proc. 1998 Intl. Conf. Biomagnetism, Sendai, Japan (Aug. 1998).

[3] Baule, G. and McFee, R., "Detection of the magnetic field of the heart," Am. Heart J., 55, p. 95 (1963)

[4] Cohen, D., Edelsack, E.A., and Zimmerman, J.E., "Magnetocardiograms taken inside a shielded room with a superconducting point-contact magnetometer," Appl. Phys. Lett., 16, p. 278 (1970).

[5] Vrba, J., et al., "Biomagnetometers for unshielded and well shielded environments," Clin. Phys. Physiol. Meas., 12B, p 81 (1991) and M. Hamalainen, et al., "Magnetoencephalography—theory, instrumentation, and applications to noninvasive studies of the working human brain," Rev. Mod. Phys., 65, p. 413 (1993)

[6] van Hulsteyn, D. B., Petschek, A. G., Flynn, E. R., and Overton, W. C. Jr., "Superconducting Imaging Surface Magnetometry", Review of Scientific Instruments 66, 3777-3784 (1995)

[7] Overton, W.C., van Hulsteyn, D.B., and Flynn, E.R., "Theoretical and experimental verification of the properties of superconductor surface imaging", IEEE Trans. on App. Superconductivity", 3, 1930-1933 (1991

[8] Cantor R, Vinetskiy V, Matlashov A, 1996, "A Low-Noise Integrated DC SQUID Magnetometer for Applications in Biomagnetism," Proc. of 10-th Intl. Conf. on Biomagnetism, Santa Fe, February 16-21, 1996.

[9] Merr, H., Purcell, A., Stroink, G., "Design of large Helmholtz Coils", Rev. Sci. Instr., 54, 7 (1983)